

# We are IntechOpen, the world's leading publisher of Open Access books Built by scientists, for scientists

6,900

Open access books available

186,000

International authors and editors

200M

Downloads

Our authors are among the

154

Countries delivered to

TOP 1%

most cited scientists

12.2%

Contributors from top 500 universities



WEB OF SCIENCE™

Selection of our books indexed in the Book Citation Index  
in Web of Science™ Core Collection (BKCI)

Interested in publishing with us?  
Contact [book.department@intechopen.com](mailto:book.department@intechopen.com)

Numbers displayed above are based on latest data collected.  
For more information visit [www.intechopen.com](http://www.intechopen.com)



# Laser Pulse Contrast Ratio Cleaning in 100 TW Scale Ti: Sapphire Laser Systems

Sylvain Fourmaux, Stéphane Payeur, Philippe Lassonde,  
Jean-Claude Kieffer and François Martin

*Institut National de la Recherche Scientifique, Énergie, Matériaux et Télécommunications -  
Université du Québec  
Canada*

## 1. Introduction

Extreme laser peak intensities can be produced with current laser technology, using both the chirped pulse amplification (CPA) technique (Strickland & Mourou, 1985) and Ti:Sapphire amplification crystals (Le Blanc et al., 1993). Laser systems using this technology are commercially providing instantaneous power in excess of 100 TW with a laser pulse duration  $\sim 30$  fs and energy per pulse of several Joules. By focusing these pulses to a few  $\mu\text{m}$  spot size, high intensity laser matter interaction studies are now routinely performed at peak intensities of  $10^{18} - 10^{20} \text{ W/cm}^2$ .

For fundamental physics research, increased laser intensities enhances current interaction processes and can lead to new and more efficient interaction regimes. A peak intensity above  $10^{22} \text{ W/cm}^2$  has already been reported by Yanovski et al. (Yanovsky et al., 2008) and a facility such as the Extreme Light Infrastructure (ELI) (Gerstner, 2007) envisions peak intensities in the range of  $10^{23} \text{ W/cm}^2$  which are needed for experiments on radiation reaction effects (Zhidkov et al., 2002).

For applications development, recent progress of laser systems combining high intensity and high repetition rate have attracted considerable interest for the production of solid target based secondary sources where high mean brightness is required. In high field science, this includes bright x-ray sources (Chen et al., 2004; Schnürer et al., 2000; Teubner et al., 2003; Thaury et al., 2007), high energy particle acceleration (Fritzler et al., 2003; Steinke et al., 2010; Zeil et al., 2010) and nuclear activation (Grillon et al., 2002; Magill et al., 2003).

To illustrate this interest for high peak intensities, recently published scaling laws for laser based proton acceleration on thin film solid targets (Fuchs et al., 2006) have shown that an important increase of the on target laser intensity is necessary to reach the expected energy required for biomedical application in the proton therapy field (60 - 250 MeV). Moreover, intensities greater than  $10^{20} \text{ W/cm}^2$  will allow access to the non collisional shock acceleration regime where  $>100$  MeV maximum energy protons could be produced (Silva et al., 2004).

For currently available peak intensities ( $10^{18} - 10^{20} \text{ W/cm}^2$  range), where the field strength is sufficient to accelerate particle to relativistic energies, the laser pulse contrast ratio (LPCR) is a crucial parameter to take into consideration. Considering the laser pulse intensity temporal profile, the LPCR is the ratio between its maximum (peak intensity) and any fixed delay before it. A low contrast ratio can greatly modify the dynamics of energy coupling between the

laser pulse and the initial target by producing a pre-plasma that can change the interaction mechanism. This issue will be even more important for future laser systems with higher intensities. Thus, LPCR characterization and improvement are of great importance for such laser systems.

In this chapter, the second section presents the basic concepts: Laser Pulse Contrast Ratio, ionization and damage thresholds definitions. Section 3 is devoted to the presentation of the typical structure and performances of a high power laser system based on CPA Ti:Sapphire technology which is currently the most popular way to reach high intensity at a high repetition rate. Section 4 presents the measurement techniques to characterize the pre-pulse, the Amplification of Spontaneous Emission (ASE), and the coherent contrast of a laser system. We can divide the pulse cleaning techniques that have been proposed to improve the LPCR into two categories: first those used before compression which mainly reduce pre-pulses and ASE; second those applied after compression which allow a coherent contrast enhancement. In the first category, we present in section 5 the technique based upon high energy injection through saturable absorbers before power amplification and the technique based on cross wave polarization (XPW). To improve the coherent contrast, only the cleaning techniques used after pulse compression are efficient (second category); we detail in section 6 the techniques of second harmonic generation and the technique using plasma mirrors. We conclude this chapter in section 7.

## 2. Basic concepts

### 2.1 Laser Pulse Contrast Ratio (LPCR) definition

We define the LPCR as the ratio  $R$  between the laser pulse peak intensity  $I_{peak}$  and any pre-pulse or pedestal intensity  $I_p$ , i.e.  $R = I_{peak}/I_p$ . A low contrast ratio laser pulse can generate a pre-plasma before the arrival of the laser pulse peak intensity and completely change the interaction mechanism between the laser pulse and the initial target (Workman et al., 1996; Zhidkov et al., 2000). For high intensity laser systems using the CPA technique, several overlapping time scales of the intensity temporal profile should be distinguished, each corresponding to a specific source of LPCR degradation (Konoplov, 2000). On the ns time scale, from a few ns up to approximately 20 ns, insufficient contrast of the amplified laser pulse relative to neighbouring pulses could occur in the oscillator or a regenerative amplifier cavity resulting in pre-pulses. Below several ns, amplified fluorescence produced by the pumped crystal during the amplification process may propagate down the amplifier system; this Amplification of Spontaneous Emission (ASE) produces a plateau shaped ns pedestal. On the ps time scale, below a few 10's of ps, imperfect pulse compression due to deficient laser spectrum manipulations results in a LPCR degradation close to the peak intensity. On this timescale, the LPCR is called the coherent contrast and corresponds to the rising edge of the laser pulse toward the peak intensity.

### 2.2 Target ionization and damage thresholds

When considering the effect of low LPCR, two target parameters are of importance: the ionization threshold and the damage threshold. The ionization threshold is intensity dependent. It corresponds to the ionization of the atomic species present in the target and production of a plasma; for example, the ionization threshold is close to  $10^{12}$  W/cm<sup>2</sup> for metals and close to  $10^{13}$  W/cm<sup>2</sup> for dielectrics targets. The presence of a pre-plasma near the target surface before the laser pulse peak intensity modifies the electron density gradient and the nature of the processes leading to laser energy absorption in the target. The damage

threshold is fluence dependent. It corresponds to the onset of a phase transition following energy deposition in the solid target and subsequent morphology change. This threshold is a function of the laser pulse duration and the nature of the target (bulk or thin film). For a low fluence, the value depends on the target material, the damage may affect only the first atomic layers such that the damage threshold may be difficult to characterize. A more precisely measured characteristic, used here, is the ablation threshold that corresponds to a strong solid to gas phase transition with ejection of matter. The ablation threshold has been covered in several papers; in metals, its value is close to a few  $\text{J}/\text{cm}^2$  for laser pulse durations of approximately 1 ns (Cabalin et al., 1998; Corkum et al., 1988). Such a morphology change certainly affects the energy absorption process and may damage or destroy the target in some cases, such as thin foils or velvet targets (Kulcsár et al., 2000).

Pre-pulses incident on the target long before the peak intensity (several ns) can modify the target surface morphology or damage it. Thus, it is absolutely necessary to check the presence of any ns pre-pulses. This measurement has to be performed before every experimental measurement set as every alignment of the laser system can detune the Pockels cells or produce reflections that can increase laser pre-pulses. Usually the duration of the pre-pulses are in the sub-ns time range, and the ablation and ionization threshold are similar.

Even if the ns pedestal is below the ionization threshold, the energy deposited over a few ns can be above the ablation threshold and can change the target morphology or damage it. Thus, it is important to check the pedestal temporal profile several ns before the laser peak intensity. A situation where the energy contained in the pedestal over a few ns is a problem is illustrated in section 5.1.

### 3. High intensity laser systems based on Ti:Sapphire technology

The architecture of a typical laser system based on CPA Ti:Sapphire technology with its amplification stages is shown in figure 1. In this example, the laser consists of: an oscillator; a grating based stretcher which increases the laser pulse duration; a regenerative amplifier; three multi-pass amplification stages to reach the final maximum laser pulse energy; and a grating compressor to restore the short laser pulse duration.

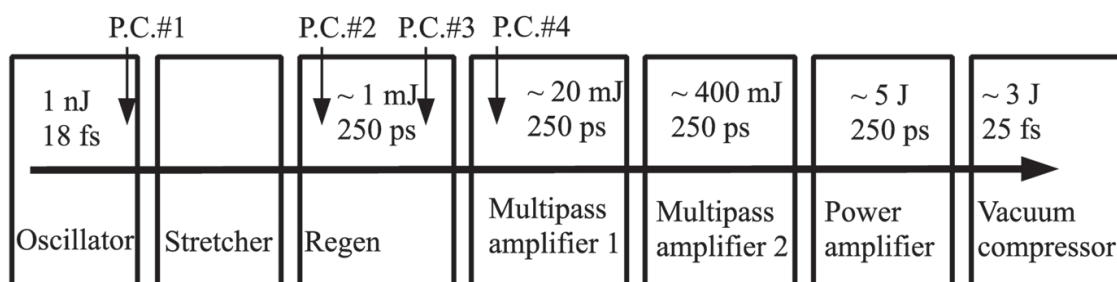


Fig. 1. Architecture of a high intensity laser system. P.C. indicates the position of the Pockels cells in the laser system. Typical output energy and pulse duration (FWHM) are indicated at each location.

The Ti:Sapphire oscillator operates at several 10's of MHz repetition rate and generates laser pulses with a central operating wavelength close to 800 nm. It typically produces an initial pulse duration of 18 fs with 80-100 nm spectral bandwidth. An acousto-optic programmable dispersive filter (AOPDF) is usually used to control the spectral phase distribution of the pulse and compensate for the gain narrowing that occurs in the different amplification stages. It is

normally placed after the stretcher to control the spectral phase and amplitude distribution of the laser pulse. The grating based stretcher increases the laser pulse duration to  $\sim 250$  ps in order to reduce the peak intensity on the optical components during the energy amplification process. A 55 nm bandwidth FWHM can typically be achieved after compression. In a typical high power laser system, the minimum pulse duration routinely produced after compression is currently 25-30 fs. Note that the grating based compressor has to be located inside a vacuum chamber as the laser pulse instantaneous power after compression on the last grating is high enough that self-focusing could occur during propagation in air leading to pulse distortion and potential damage to the optics.

The regenerative cavity provides a high amplification factor of  $10^5 - 10^6$ . Note that some laser systems do not use a regenerative amplifier but only multi-pass amplifiers (Pittman et al., 2002). In our example, the output energy of the first two multi-pass amplifiers is approximately 20 mJ and 400 mJ, respectively. The final amplification stage increases the laser pulse energy up to several Joules. This amplifier usually includes a large number of YAG pump laser, each typically providing close to 1 J in energy. The amplification crystals are usually water cooled except for the final stage which requires cryogenic cooling to avoid thermal lensing. As an example, a 30 fs laser pulse with an output energy of 3 J after compression corresponds to an instantaneous power of 100 TW.

Pockels cells are used through the laser system to isolate the main pulse and increase the LPCR: the first, the pulse picker reduces the laser repetition rate from the MHz range down to the Hz range; the second, at the entrance of the regenerative cavity, serves to seed it; the third, inside the regenerative cavity, allows the amplified pulse to exit and the fourth, between the regenerative cavity and the first multi-pass amplifier, reduces the pre-pulse level. These Pockels cells rotate the polarization and effectively isolate the amplified laser pulse with a typical switching time of approximately 4 ns. For a laser system with a power greater than 10 TW up to a few 100's of TW, the laser repetition rate is typically 10 Hz.

We can illustrate the architecture of a high intensity laser with the performance of a commercially available system based on CPA Ti:Sapphire technology. The technical specifications of the 10 TW laser system of the Advanced Laser Light Source (ALLS) facility located in Varennes (Canada) are the following: the minimum pulse duration is 32 fs, limited by the gain narrowing occurring during the amplification; only two multi-pass amplifiers are used, providing 400 mJ before compression; the repetition rate is 10 Hz and the central wavelength is 800 nm.

## **4. Laser Pulse Contrast Ratio measurements techniques**

### **4.1 Pre-pulse measurement by a fast photodiode**

The pre-pulses in the nanosecond time range are usually detected at the nominal laser energy using the leakage through a high reflectivity mirror. A fast photodiode (typically a high-speed silicon photodiode with 1 ns rise time) coupled to neutral density (ND) filters calibrated at the laser wavelength are used to measure the ns pre-pulses. As the photodiode rise time is greater than the duration of any typical pre-pulse, the measured value corresponds to the integrated pre-pulse energy; it is important to measure the pre-pulse duration separately to determine its intensity and associated LPCR. Normally, the time delay between the pre-pulses and the peak intensity is fixed by the round trip time of the oscillator and the regenerative amplifier which is typically from a few ns up to 10's of ns.

Again using the ALLS facility 10 TW laser system as example, the pre-pulses are generated by the regenerative amplifier cavity at 8 ns before the peak intensity of the laser pulse. The

time delay between these pre-pulses and the main amplified pulse is a multiple of a round trip inside the regenerative cavity, the first pre-pulse exits the cavity before the main pulse with one less round trip. The typical energy ratio between the amplified pulse maximum energy and the first pre-pulse is  $3 \times 10^4$ . The first pre-pulse duration is 500 fs corresponding to a LPCR of  $4.7 \times 10^5$ . The use of an additional Pockels cell after the regenerative cavity increases the LPCR of the pre-pulses by a factor 60 but has no effect on shorter timescales because of the limited rise time of the Pockels cells.

#### 4.2 ASE and coherent contrast measurement using a high dynamic range third-order cross-correlator

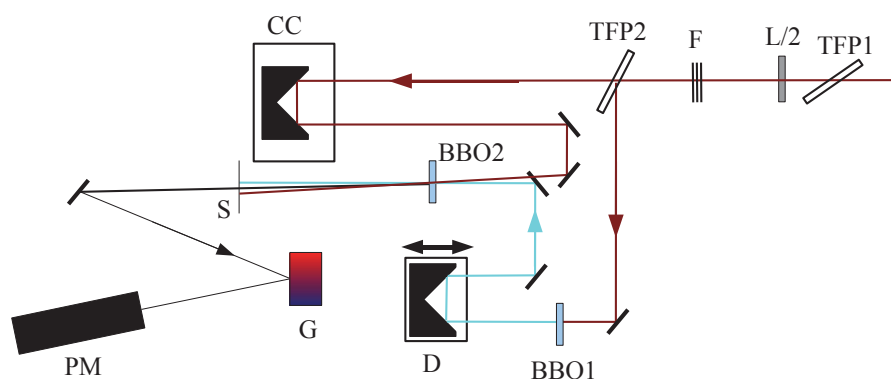


Fig. 2. Experimental set-up for LPCR measurement of the laser system pulse pedestal and coherent contrast using a high dynamic range third order cross-correlator. The arrows illustrate the laser beam propagation path, the 800 nm beam is indicated in red, the 400 nm (second harmonic) in blue, and the 266 nm (third harmonic) in black. TFP1 and TFP2 are thin film polarizer, F is a set of calibrated filters, L/2 is a wave-plate; BBO1 and BBO2 are BBO crystals, D is a motorized delay line and CC is a corner cube, S is a slit to select the third harmonic beam, G a grating and PM the photo-multiplier detector.

The LPCR for the time range of a few ns is characterized using a high dynamic range third-order cross-correlator. For this measurement, part of the laser beam is usually sampled while the laser system is working at nominal energy or close to it. During the measurement, the last amplification stage can only be partly pumped, this does not significantly affect the final result as long as most of the amplification has been obtained (Kiriya et al., 2010). The experimental set-up is described on figure 2. The sampled beam is divided using a polarizer beamsplitter (TFP2). The reflected part is frequency doubled using a 200  $\mu\text{m}$  thick type I BBO crystal and reflected by a motorized delay line (D). The transmitted part at the fundamental frequency is directed toward a corner cube (CC). Both beams are then combined in a non-collinear geometry into a 100  $\mu\text{m}$  thick type II BBO crystal to generate the third harmonic. The 266 nm third harmonic is separated from the other wavelengths using a grating and recorded by a photomultiplier.

The use of calibrated neutral density filters allows the cross-correlator to cover a dynamic range typically of 12 decades. The range of the motorized delay line (D) is limited to 600 ps in the standard commercial cross-correlator. In routine use, usually only the pedestal

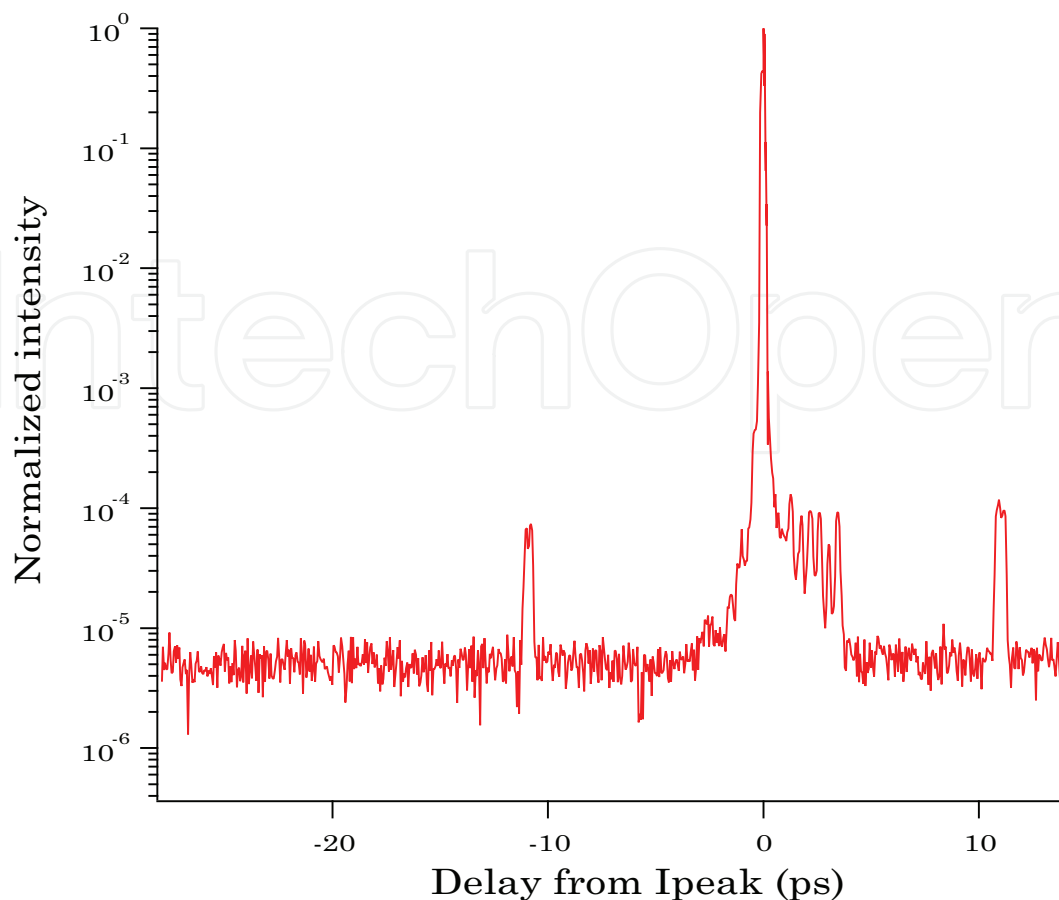


Fig. 3. Normalized intensity (inverse of LPCR) for the time interval ranging before the laser pulse peak intensity from -28 ps up to +14 ps. Courtesy of A. Laramée and F. Poitras of the ALLS facility technical team.

level several 10's of ps before the peak amplified laser pulse and the rising edge of the laser pulse are checked. The corner cube (CC) can be set onto a second manual delay line to allow successive scans with different offset values to cover delays greater than 600 ps between the fundamental and the second harmonic. The pedestal has been studied in this way in the ns range (Fourmaux et al., 2011; Hong et al., 2005; Itatani et al., 1998). The background level limits the dynamic range over which the measurement can be achieved. This is determined by blocking the fundamental frequency on the transmitted part of the beam. It should also be mentioned that the cross-correlator measurement increases the pulse duration up to  $\sim 100$  fs due to pulse dispersion by the vacuum window, filters and BBO crystals used in the cross-correlator and to sample the beam. Several pre-pulses are usually observed before the main pulse (see in figure 3 the pre-pulse at -10 ps). These correspond to replica of post pulses due to the presence of windows or optics in the laser system and the cross-correlator diagnostic (the 266 nm third harmonic results from a convolution of the 800 nm fundamental wavelength by the 400 nm second harmonic).

Using the ALLS facility 10 TW laser system as example, figure 3 shows the normalized intensity for a time interval before the laser peak intensity of -28 ps up to 14 ps. The LPCR due to the pedestal level is  $2 \times 10^5$ . Assuming a solid metallic target, a focused intensity of  $5 \times 10^{17}$  W/cm<sup>2</sup> is then high enough to ionize the target. This clearly demonstrates that standard high power laser systems need to improve the LPCR in order to avoid pre-plasma production.

## 5. Pulse cleaning techniques for ultrafast laser system

Several techniques have been proposed in order to enhance the LPCR in ultrafast CPA laser system: saturable absorbers (Hong et al., 2005; Itatani et al., 1998), double CPA laser system (Kalashnikov et al., 2005), non linear birefringence (Jullien et al., 2004), cross polarized wave generation (XPW) (Petrov et al., 2007), plasma mirror (Lévy et al., 2007) or second harmonic generation (Toth et al., 2007). Details of these techniques can be found in the cited references. Few of these pulse cleaning techniques have been implemented in high repetition rate 100 TW scale laser systems and usually, the LPCR have only been characterized to a few 100 ps before the laser pulse peak intensity. This section covers the cleaning techniques used before compression, these mainly reduce pre-pulses and ASE on high intensity Ti:Sapphire laser system. The following section will cover the cleaning techniques used after compression.

### 5.1 Saturable absorber cleaning and high energy injection before power amplification

This cleaning technique is based on removing the pedestal through saturable absorber transmission and high energy injection before power amplification. A saturable absorber is an optical component with a high optical absorption which is reduced at high intensities. As the intensity of the pedestal and any pre-pulses is not intense enough to change the absorption of the saturable absorber, they are not transmitted. But the high intensity portion of the laser pulse will trigger a change in absorption on its rising edge, enhancing the laser pulse temporal contrast ratio for the transmitted laser pulse. This technique has been applied previously to low power laser systems (Hong et al., 2005; Itatani et al., 1998) and is now applied with 100 TW class CPA laser systems, producing an LPCR of  $10^8$ - $10^9$ .

The Canadian ALLS 200 TW laser system uses such a saturable absorber to improve the LPCR before injection into the regenerative amplifier. This laser system produces 25 fs pulses with an energy of 5.4 J after compression at a 10 Hz repetition rate. The maximum intensity obtained with a f/3 off axis parabola is  $3 \times 10^{20}$  W/cm<sup>2</sup> (Fourmaux et al., 2008). The cleaning stage, located between the oscillator and the stretcher, consists of a 14 pass ring amplifier pumped with 8 mJ of energy, followed by a 2 mm thick RG 850 saturable absorber used to increase the LPCR at this stage of amplification. The laser pulse energy after the cleaning stage is 10  $\mu$ J, the gain amplification factor is  $10^4$  and the saturable absorber transmission is 45%. The fluence in the saturable absorber is 10 mJ/cm<sup>2</sup>. This allows the injection of a pre-amplified laser pulse with a high LPCR, reducing the required subsequent amplification and hence decreasing ASE production.

The normalized intensity of the laser system is shown in figure 4 for a time delay before  $I_{peak}$  ranging from -5.4 ns up to +100 ps. This measurement is achieved, using the third order cross-correlator, by setting the corner cube (CC) onto a manual delay line and moving it several times in order to achieve a time delay up to 5.4 ns before  $I_{peak}$ . The LPCR exhibits a minimum 55 ps before  $I_{peak}$  at  $10^9$ , increasing for longer delays; for example, the LPCR is  $2.5 \times 10^8$  at -500 ps. The inset in figure 4 shows the normalized intensity for a time delay before  $I_{peak}$  ranging from -500 up to +100 ps; this is basically the coherent contrast. Small bumps with a 500-600 ps periodicity can be observed in figure 4. These correspond to a reproducible instrument artifact from an angular shift that occurs at the centre of the motorized translation's travel (delay line D). This does not affect the aspect of the ASE signal.

There is a general deterioration of the LPCR for increasing delays before  $I_{peak}$ , especially in the interval between 250 ps and 2.1 ns with a value close to  $2.5 \times 10^8$ . We attribute this trend to the ASE generated inside the regenerative amplification. Indeed, during this delay range,

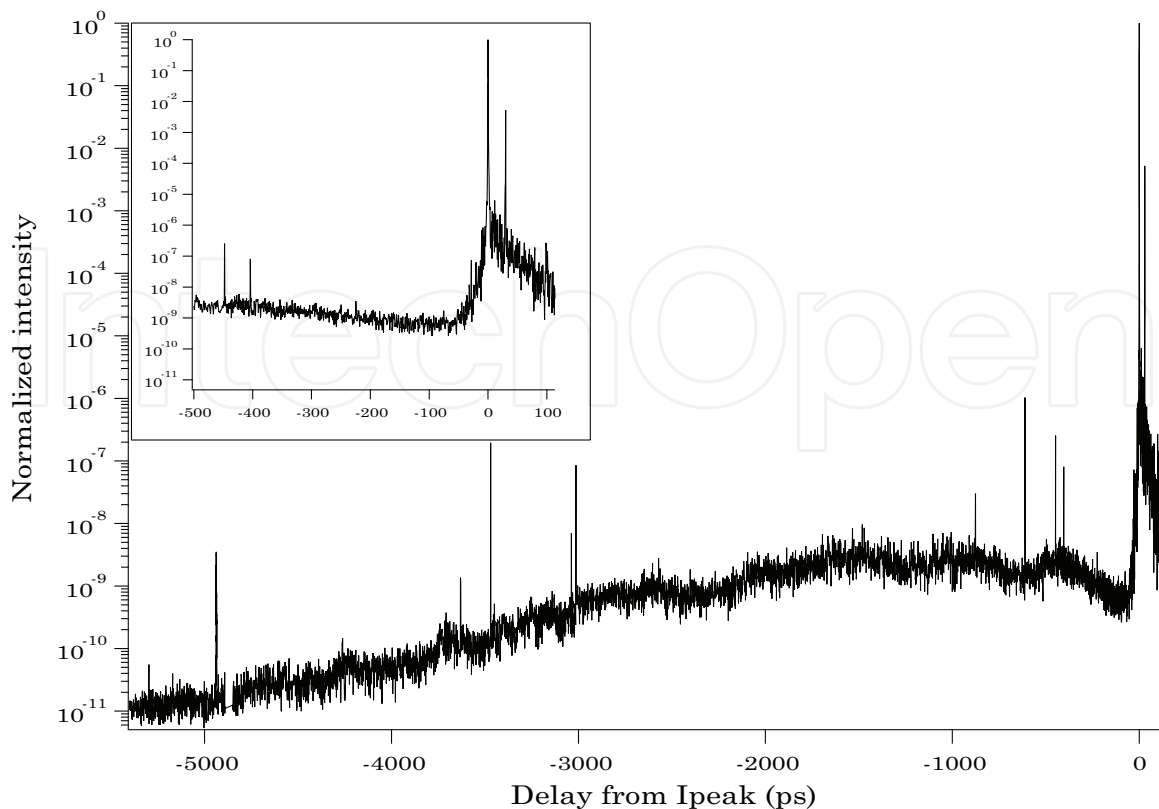


Fig. 4. Normalized intensity (inverse of LPCR) for large delays before the laser pulse peak intensity up to 5.4 ns. The inset shows a magnification of the time interval ranging from -500 ps up to +100 ps.

the amplification is sufficiently high to produce an important amount of ASE. During the amplification process, injecting the chirped laser pulse temporally decreases the ASE. For an amplifier in the saturation regime, this occurs because of the competition between the ASE and the stretched pulse to deplete the population of excited states. As the number of photons is greater in the chirped pulse compared to ASE, this depletion occurs to the detriment of the ASE. This explains why the LPCR remains high for delays close to the amplified laser pulse. Considering this LPCR, a maximum peak intensity of  $2.5 \times 10^{20} \text{ W/cm}^2$  is acceptable for the pedestal intensity to remain below the ionization threshold  $10^{12} \text{ W/cm}^2$ . Taking into account the correction factor due to the pulse broadening increases this intensity to  $2 \times 10^{21} \text{ W/cm}^2$ ; this is greater than the maximum peak intensity that can be reached by such a laser system with a  $f/3$  off-axis parabola. Thus with these focusing conditions the LPCR is high enough to avoid pre-plasma production on target before the rising edge of the laser pulse. However, the energy deposited before the peak intensity must also remain below the ablation threshold ( $1 \text{ J/cm}^2$ ). Due to the LPCR degradation a few ns before the peak laser intensity, this limits the peak intensity to  $1.7 \times 10^{18} \text{ W/cm}^2$ , well below the maximum intensity that can be obtained with this laser system. Thus, even though the LPCR is  $10^9$  a few 10's of ps before the peak laser intensity, the ASE of this laser system is an issue. A simple method to reduce the ASE in this system has been proposed: it consists of adding an additional saturable absorber after the regenerative cavity in order to reduce the pre-pulses and the pedestal (Fourmaux et al., 2011).

## 5.2 XPW technique

XPW generation is a third order non-linear process that rotates the polarization of the laser pulse; the intensity of the rotated pulse is cubic with the input intensity. Thus XPW generation is well adapted for enhancing the LPCR of a femtosecond laser pulse. When used between crossed-polarizers, XPW generation rejects the low-intensity parts of the pulse to improve the LPCR. A barium fluoride (BaF<sub>2</sub>) nonlinear crystal is usually used for XPW generation. Details of the XPW technique and research related to the prospects of its implementation on high power laser system can be found in several publications (Cotel et al., 2006; Jullien et al., 2004; Jullien, Albert et al.;K; Ramirez et al., 2011).

Techniques using XPW generation have been implemented in a double CPA geometry on a few 10 TW class laser system: "salle jaune" (10 Hz, 1.5 J, 30 fs) at LOA (Flacco et al., 2010) and LOASIS laser system (10 Hz, 500 mJ, 40 fs) at LBNL (Plateau et al., 2009), but except for measurements in the ps time range, no detailed characterization of the LPCR is available.

The XPW technique has also been implemented on the HERCULES laser at CUOS without the use of an additional CPA. To achieve this, a higher input energy (1  $\mu$ J) is used for XPW generation in two BaF<sub>2</sub> crystals mounted in series with an AOPDF to compensate for the dispersion in the optics. The laser system produces after 1.5 J of energy in a 30 fs pulse after compression at a 0.1 Hz repetition rate (Chvykov et al., 2006).

Their measurement indicate an LPCR improvement of 3 orders of magnitude for the pedestal level at a few hundred ps before the peak intensity. Chvykov et al. have demonstrated an LPCR of  $10^{11}$  using XPW in this single CPA geometry. No detailed characterization on the ns range is presented in their work and the low repetition rate allows only 0.15 W of average power, insufficient for high brightness laser based applications. According to the authors, this LPCR level is high enough to work with a laser pulse focused to an on target intensity of  $10^{22}$  W/cm<sup>2</sup> and avoid pre-plasma production.

## 6. Coherent contrast improving cleaning techniques

The previously described techniques are used to clean the laser pulse before compression. Thus, they do not improve the coherent contrast which is limited by the imperfect pulse compression associated with deficient manipulations of the laser spectrum. Steepening the rising edge of the laser pulse is important for laser generated processes such as proton acceleration or harmonics generation on solid targets, to properly control the laser plasma interaction (Grismayer & Mora, 2006; Teubner et al., 2003). Using a cleaning technique after compression is challenging for high power laser systems as an energy level of several Joule precludes the use of standard transmission optical components.

### 6.1 Second harmonic generation

This technique is commonly used on high power laser systems with longer pulse durations, from 100's of fs to ns (using Nd:glass amplification crystals), because high conversion efficiencies are easily attained using non-linear crystals such as KDP (potassium dihydrogen phosphate), KD\*P (potassium dideuterium phosphate), BBO ( $\beta$ -barium borate) or LBO (lithium triborate). For example, close to 70 % second harmonics conversion efficiency can be obtained using a 1054 nm laser pulse with ps pulse duration into a KDP crystal of a few mm length at a laser intensity of  $100$  GW/cm<sup>2</sup> (Amiranoff et al., 1999).

Second harmonic generation is more difficult for Ti:Sapphire high power laser systems with pulse durations between 25 - 60 fs and an energy of several Joule ( Begishev et al., 2004; Marcinkevicius et al., 2003). A very short pulse duration requires that a thin doubling crystal

be used because of the group velocity mismatch between the fundamental and the second harmonic wavelength at 800 and 400 nm respectively. For example, group velocity mismatch limits the optimum KDP crystal thickness to  $600\ \mu\text{m}$  for a 50 fs laser pulse duration, reducing the length over which efficient second harmonic generation can occur.

Usually, when considering high power laser system with large beams operated under vacuum after compression, it is easier to directly propagate the beam in the doubling crystal instead of using an afocal system, with optical components in reflection, to reduce the beam diameter. Another reason to keep the beam diameter large is to keep a sufficiently low laser intensity to avoid self phase modulation effects that decreases the conversion efficiency and distorts the beam wavefront. Using a laser system with 3 J of energy, 90 mm beam diameter at full aperture is typical. Today, the only crystal that can be found with such large dimensions is KDP.

Moreover, the second harmonics crystal must not distort the wavefront to avoid degraded beam focusing, thus requiring good optical quality surfaces. Unfortunately, the larger diameter crystal require a greater thickness to maintain a good optical quality: for example, 1 mm thickness for a 100 mm full aperture diameter KDP crystal. Another problem with using a very short pulse duration is the frequency bandwidth; a typical bandwidth of 80 nm is necessary to obtain a 25 fs laser pulse duration. The second harmonic generation will remain efficient as long as the phase matching conditions are satisfied. This occurs only over a limited range of wavelength, thus reducing the effective bandwidth.

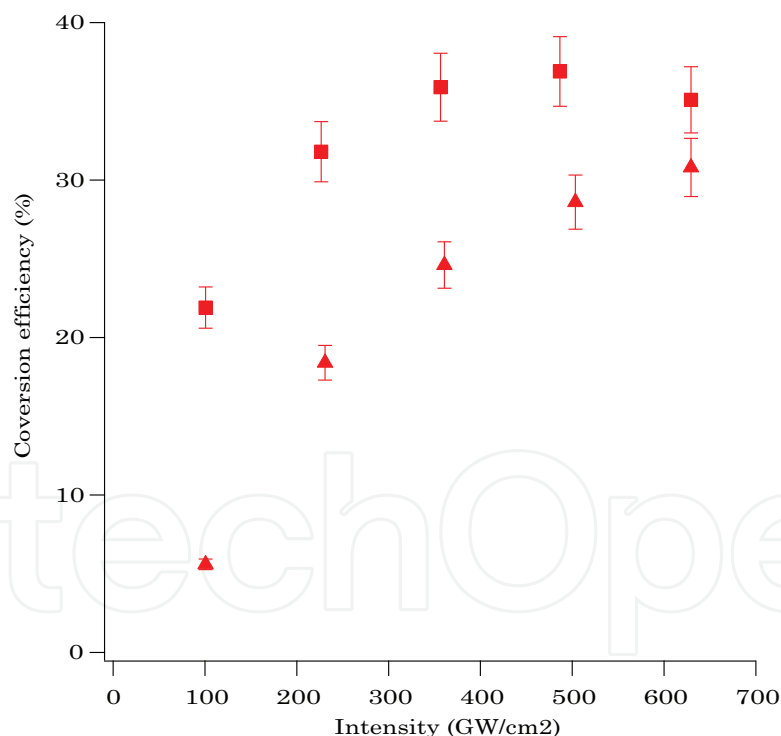


Fig. 5. Second harmonic conversion efficiency as a function of the intensity on the KDP doubling crystal using the 10 TW ALLS laser system. The results have been obtained with two crystals thickness: 1mm (square) and  $600\ \mu\text{m}$  (triangle).

The optimum conversion efficiency has been measured as a function of the incident energy using a KDP doubling crystal with the 10 TW ALLS laser system having a 32 fs laser pulse duration. The result is shown on figure 5 for two crystal dimensions: 1 mm thick  $\times$  60

mm diameter (square) and  $600\ \mu\text{m}$  thick  $\times$  40 mm diameter (triangle). Note that the pulse duration has been optimized for each crystal thickness in order to obtain the maximum conversion efficiency (the pulse duration was set by changing the optical distance between the compression gratings). The maximum energy used in this measurement for both KDP crystals thickness is 180 mJ after compression.

This cleaning technique has been used with the INRS 10 TW laser system in order to limit the hydrodynamic plasma expansion when laser pulses were focused on solid target to produce  $K\alpha$  x-ray line emission; the laser system was producing 60 fs pulses of 600 mJ energy per pulse at a 10 Hz repetition rate. In this particular case, the contrast ratio at the fundamental frequency was close to  $10^5$ , for both the picosecond and the nanosecond time range. In these experiments, the beam was frequency doubled with a KDP crystal to achieve a high contrast ratio exceeding  $10^9$ . A good beam quality was maintained at 400 nm in the near and far field. A conversion efficiency of 40% was achieved using a 1 mm thick KDP crystal. This reduces the available energy before focusing down to 200 mJ but maintains the repetition rate without any limitation in the number of pulses (Toth et al., 2005; 2007).

When a sufficiently high conversion efficiency is achieved, the advantages of this techniques, are that it maintains the nominal repetition rate of the laser system and improves the LPCR (square of the initial value) while requiring only a relatively simple experimental setup (direct propagation inside the doubling crystal is enough). It should be pointed out that, when frequency doubling the laser pulse, a large fraction of the energy remains at the fundamental frequency. To take full advantage of the LPCR improvement of the second harmonic, the 400 nm wavelength has to be discriminated from the 800 nm wavelength as this last one arrives in advance in time compare to the 400 nm wavelength (usually this is realized by using several dichroic mirrors). The drawbacks of this technique are the low conversion efficiency because of unadapted crystal (for lack of availability) and the difficulty in obtaining the optimum phase matching conditions.

## 6.2 Plasma mirror

The principle of the plasma mirror is shown in figure 6: a glass plate with an anti-reflection coating is inserted at  $45^\circ$  into the converging laser beam, after the the focusing optics (typically an off-axis parabola) and a few mm before the laser focus. The laser fluence on the plasma mirror is approximately  $100\ \text{J}/\text{cm}^2$ , corresponding to a peak intensity of  $10^{15}$ - $10^{16}\ \text{W}/\text{cm}^2$

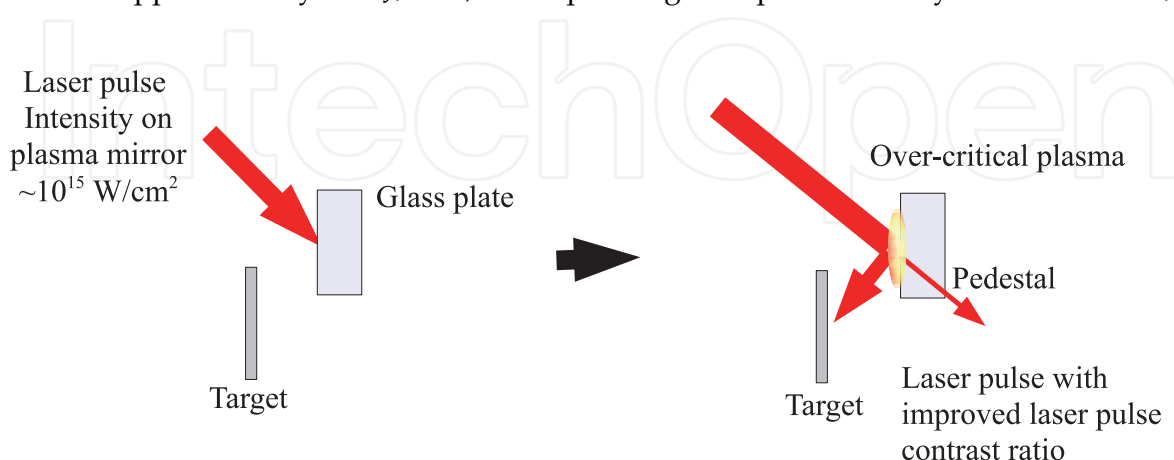


Fig. 6. Principle of the plasma mirror in the case of a simple geometry close to the target.

on the plate (considering a 30 fs pulse duration). Such an intensity generates a solid-density plasma on the glass plate surface, reflecting the laser pulse at its critical density. Since the laser pedestal and any pre-pulses are not intense enough to produce dielectric breakdown, these are not reflected and propagate through the plate. There is thus an enhancement of the laser pulse temporal contrast ratio (LPCR) for the reflected laser pulse. The plasma mirror is laterally translated after each shot to present a fresh surface for the next shot. The advantage of such a technique is to reduce both the pre-pulse, ASE and rising front of the laser pulse.

Several groups have developed plasma mirror systems (Doumy et al., 2004; Dromey et al., 2004; Hörlein et al., 2008; Nomura et al., 2007; Wittmann et al., 2006).

A double plasma mirror geometry has been implemented on a 10 TW laser system at CEA-Saclay. This laser nominally produces 60 fs pulses with 700 mJ energy at a 10 Hz repetition rate. Implementing the plasma mirror reduces the repetition rate to 1 Hz with a total reflectivity of 50 % and a total shot number limited to 2000 (Thaury et al., 2007).

## 7. Conclusion

Characterization and improvement of the LPCR is a crucial problem for laser plasma interaction on solid targets as ultra-short laser systems delivering increasing energy and peak intensity become available. Several techniques are available to control the laser-target interaction to avoid damaging the target or producing a pre-plasma, but none of these can compensate all the different causes of LPCR degradation (pre-pulses, ASE and rising edge of the laser front) with good efficiency while maintaining the laser repetition rate. For the study of basic physics processes, the plasma mirror has proven to be an important tool but its implementation is non trivial and the limited number of shots available prevents its applications outside the field of basic research. The two more widespread techniques used today on commercial high intensity laser system, XPW and high energy injection after a saturable absorber, do not improve the coherent contrast. Moreover, the pre-pulses or the ASE level have to be checked carefully so they remain low enough not to affect the interaction conditions.

Improvement of these techniques is still an active area of research both for the use of high intensity laser system in the field of fundamental physics studies and for the development of technological applications. Until now, LPCR reduction techniques are clearly advantaged for laser based process and applications using gas targets since the requirements are important but not critical as for solid targets.

## 8. Acknowledgment

We thank the ALLS technical team for their support, especially F. Poitras and A. Laramée for their help on the ALLS 10 TW laser system characterization. The ALLS facility was funded by the Canadian Foundation for Innovation (CFI). This work was funded by NSERC, the Canada Research Chair program and Ministère de l'Éducation du Québec.

## 9. References

- F. Amiranoff, V. Malka, M. Salvati, E. L. Clark, A. E. Dangor, K. Krushelnick, A. Modena, Z. Najmudin, M. I. Santala, M. Tatarakis *et al.*, (1999). Electron acceleration in a pre-formed plasma at 527 nm : an experiment performed with funding from the TMR large-scale facilities access programme. RAL *Technical report*, RAL-TR-99-008

- I. A. Begishev, M. Kalashnikov, V. Karpov, P. Nickles, H. Schönagel, I. A. Kulagin & T. Usmanov (2004). Limitation of second-harmonic generation of femtosecond Ti:sapphire laser pulses *J. Opt. Soc. Am. B*, Vol. 21, pp. 318-322
- L.M. Cabalin & J. J. Laserna, (1998). Experimental determination of laser induced breakdown thresholds of metals under nanosecond Q-switched laser operation *Spectrochimica Acta Part B*, Vol. 53, pp. 723-730
- L. M. Chen, P. Forget, S. Fourmaux *et al.*, (2004). Study of hard x-ray emission from intense femtosecond Ti:Sapphire laser-solid target interactions *Phys. of Plasmas*, Vol. 11, pp. 4439
- V. Chvykov, P. Rousseau, S. Reed, G. Kalinchenko & V. Yanovsky, (2006). Generation of 1011 contrast 50 TW laser pulses *Opt. Lett.*, Vol. 31, pp. 1456-1458
- P. B. Corkum, F. Brunel, N. K. Sherman & T. Srinivasan-Rao, (1998). Thermal Response of Metals to Ultrashort-Pulse Laser Excitation *Phys. Rev. Lett.*, Vol. 61, pp. 2886-2889
- A. Cotel, A. Jullien, N. Forget, O. Albert, G. Chériaux & C. Le Blanc, (2006). Nonlinear temporal pulse cleaning of a 1- $\mu\text{m}$  optical parametric chirped-pulse amplification system *Appl. Phys. B*, Vol. 83, pp. 7
- G. Doumy, F. Quéré, O. Gobert, M. Perdrix, Ph. Martin, P. Audebert, J. C. Gauthier, J.-P. Geindre & T. Wittmann (2004). Complete characterization of a plasma mirror for the production of high-contrast ultraintense laser pulses *Phys. Rev. E*, Vol. 69, pp. 026402-12
- B. Dromey, S. Kar, M. Zepf & P. Foster (2004). The plasma mirror: subpicosecond optical switch for ultrahigh power lasers *Rev. Sci. Instrum.*, Vol. 75, pp. 645-649
- A. Flacco, T. Ceccotti, H. George, P. Monot, Ph. Martin, F. Réau, O. Tcherbakoff, P. d'Oliveira, F. Sylla, M. Veltcheva, F. Burgy, A. Tafzi, V. Malka & D. Batani, (2010). Comparative study of laser ion acceleration with different contrast enhancement techniques *Nuclear Instruments and Methods in Physics Research Section A*, Vol. 620, pp. 18-22
- S. Fourmaux, S. Payeur, A. Alexandrov, C. Serbanescu, F. Martin, T. Ozaki, A. Kudryashov & J. C. Kieffer, (2008). Laser beam wavefront correction for ultra high intensities with 100 TW laser system at the Advanced Laser Light Source *Opt. Express*, Vol. 16, pp. 11987
- S. Fourmaux, S. Payeur, S. Buffechoux, P. Lassonde, C. St-Pierre, F. Martin & J. C. Kieffer, (2011). Pedestal cleaning for high laser pulse contrast ratio with a 100 TW class laser system *Opt. Express* Vol. 19, pp. 8486-8497
- S. Fritzler, V. Malka, G. Grillon, J. P. Rousseau, F. Burgy, E. Lefebvre, E. d'Humières, P. McKenna & K. W. D. Ledingham, (2003). Proton beams generated with high-intensity lasers: Applications to medical isotope production *Appl. Phys. Lett.*, Vol. 83, pp. 3039
- J. Fuchs, P. Antici, E. d'Humières *et al.*, (2006). Laser-driven proton scaling laws and new paths towards energy increase *Nature Physics*, Vol. 2, pp. 48
- E. Gerstner, (2007). Laser physics: Extreme light *Nature*, Vol. 446, pp. 16 - 18
- G. Grillon, Ph. Balcou, J.- P. Chambaret, D. Hulin, J. Martino, S. Moustazis, L. Notebaert, M. Pittman, Th. Pussieux, A. Rousse, J- Ph. Rousseau, S. Sebban, O. Sublemontier & M. Schmidt (2002). Deuterium-Deuterium Fusion Dynamics in Low-Density Molecular-Cluster Jets Irradiated by Intense Ultrafast Laser Pulses *Phys. Rev. Lett.*, Vol. 89, pp. 065005
- T. Grismayer & P. Mora, (2006). Influence of a finite initial ion density gradient on plasma expansion into a vacuum *Physics of Plasmas*, Vol. 13, pp. 032103-7

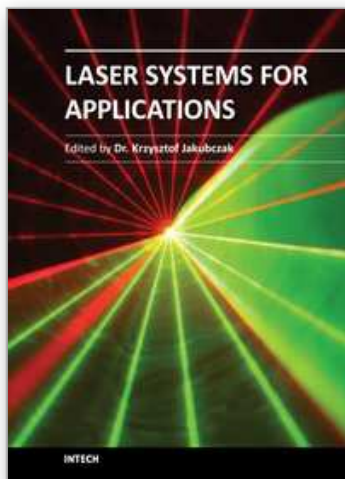
- K.-H. Hong, B. Hou, J.A. Nees, E. Power & G.A. Mourou, (2005). Generation and measurement of >108 intensity contrast ratio in a relativistic kHz chirped-pulse amplified laser *Appl. Phys. B* Vol. 81, pp. 447-457
- R. Hörlein, B. Dromey, D. Adams, Y. Nomura, S. Kar, K. Markey, P. Foster, D. Neely, F. Krausz, G. D. Tsakiris & M. Zepf, (2008). High contrast plasma mirror: spatial filtering and second harmonic generation at  $10^{19}$  W cm<sup>2</sup> *New Journal of Physics*, Vol. 10, pp. 083002-12
- J. Itatani, J. Faure, M. Nantel, G. Mourou & S. Watanabe, (1998). Suppression of the amplified spontaneous emission in chirped-pulse-amplification lasers by clean high-energy seed-pulse injection *Optics Communications* Vol. 148, pp. 70-74
- A. Jullien, F. Augé-Rochereau, G. Chériaux, J.-P. Chambaret, P. d'Oliveira, T. Auguste & F. Falcoz, (2004). High-efficiency, simple setup for pulse cleaning at the millijoule level by nonlinear induced birefringence *Opt. Lett.*, Vol. 29, pp. 2184-2186
- A. Jullien, O. Albert, G. Chériaux, J. Etchepare, S. Kourtev, N. Minkovski & S. M. Satiel, (2006). Two crystal arrangement to fight efficiency saturation in cross-polarized wave generation *Opt. Express*, Vol. 14, pp. 2760
- A. Jullien, S. Kourtev, O. Albert, G. Chériaux, J. Etchepare, N. Minkovski & S. M. Satiel, (2006). Highly efficient temporal cleaner for femtosecond pulses based on cross-polarized wave generation in a dual crystal scheme *Appl. Phys. B*, Vol. 84, pp. 409-414
- M. P. Kalashnikov, E. Risse, H. Schonnagel & W. Sandner, (2005). Double chirped-pulse-amplification laser: a way to clean pulses temporally *Optics Lett.*, Vol. 30, pp. 923-925
- H. Kiriya, M. Mori, Y. Nakai, T. Shimomura, H. Sasao, M. Tanoue, S. Kanazawa *et al.*, (2010). High temporal and spatial quality petawatt-class Ti:sapphire chirped-pulse amplification laser system *Opt. Lett.*, Vol. 35, pp. 1497-1499
- O. A. Konoplov, (2000). Temporal high-contrast structure of ultrashort pulses: a plea for standardization of nomenclature and conventions *Proc. of SPIE*, Vol. 3934, pp. 102-112
- G. Kulcsár, D. Al Mawlawi, F. W. Budnik, P. R. Herman, M. Moskovits, L. Zhao & R. S. Marjoribanks, (2000). Intense Picosecond X-Ray Pulses from Laser Plasmas by Use of Nanostructured 'Velvet' Targets *Phys. Rev. Lett.*, Vol. 84, pp. 5149-5152
- C. Le Blanc, G. Grillon, J. P. Chambaret, A. Migus & A. Antonetti, (1993). Compact and efficient multipass Ti:sapphire system for femtosecond chirped-pulse amplification at the terawatt level *Opt. Lett.*, Vol. 18, pp. 140-142
- A. Lévy, T. Ceccotti, P. d'Oliveira, F. Réau, M. Perdrix, F. Quéré, P. Monot, M. Bougeard, H. Lagarde, P. Martin, J.-P. Geindre & P. Audebert, (2007). Double plasma mirror for ultrahigh temporal contrast ultraintense laser pulses *Opt. Lett.*, Vol. 32, pp. 310-312
- J. Magill, H. Schwoerer, F. Ewald *et al.*, (2003). Laser transmutation of iodine-129 *Appl. Phys. B*, Vol. 77, pp. 387
- A. Marcinkevičius, R. Tommasini, G.D. Tsakiris, K.J. Witte, E. Gaižauskas & U. Teubner (2004). Frequency doubling of multi-terawatt femtosecond pulses *Applied Physics B*, Vol. 79, pp. 547-554
- Y. Nomura, L. Veisz, K. Schmid, T. Wittmann, J. Wild & F. Krausz, (2007). Time-resolved reflectivity measurements on a plasma mirror with few-cycle laser pulses *New Journal of Physics*, Vol. 9, pp. 9
- G. I. Petrov, O. Albert, J. Etchepare & S. M. Satiel, (2001). Cross-polarized wave generation by effective cubic nonlinear optical interaction *Opt. Lett.*, Vol. 26, pp. 355-357

- M. Pittman, S. Ferré, J. P. Rousseau, L. Notebaert, J. P. Chambaret, & G. Chériaux, (2002). Design and characterization of a near-diffraction-limited femtosecond 100-TW 10-Hz high-intensity laser system *Appl. Phys. B*, Vol. 74, pp. 529
- G. R. Plateau, N. H. Matlis, O. Albert, C. Tóth, C. G. R. Geddes, C. B. Schroeder, J. van Tilborg, E. Esarey & W. P. Leemans, (2009). Optimization of THz Radiation Generation from a Laser Wakefield Accelerator *Proceedings of Advanced Accelerator Concepts: 13th Workshop*, CP1086, edited by C. B. Schroeder, W. Leemans and E. Esarey, AIP, pp. 707-712
- L. P. Ramirez, D. N. Papadopoulos, A. Pellegrina, P. Georges, F. Druon, P. Monot, A. Ricci, A. Jullien, X. Chen, J. P. Rousseau & R. Lopez-Martens, (2011). Efficient cross polarized wave generation for compact, energy-scalable, ultrashort laser sources *Optics Express*, Vol. 19, pp.93-98
- M. Schnürer, R. Nolte, A. Rousse *et al.*, (2000), Dosimetric measurements of electron and photon yields from solid targets irradiated with 30 fs pulses from a 14 TW laser *Phys. Rev. E*, Vol. 61, pp. 4394
- L. O. Silva, M. Marti, J. R. Davies *et al.*, (2004). Proton Shock Acceleration in Laser-Plasma Interactions *Phys. Rev. Lett.*, Vol. 92, pp. 015002
- S. Steinke, A. Henig, M. Schnurer, T. Sokollik, P.V. Nickles, D. Jung, D. Kieffer, R. Horlein, J. Schreiber, T. Tajima, X.Q. Yan, M. Hegelich, J. Meyer-Ter-Vehn, W. Sandner & D. Habs (2010). Efficient ion acceleration by collective laser-driven electron dynamics with ultra-thin foil targets *Laser and Particle Beams*, Vol. 28, pp. 215-221
- D. Strickland & G. Mourou, (1985). Compression of amplified chirped optical pulses *Optics Communications*, Vol. 55, pp. 447-449
- U. Teubner, G. Pretzler, Th. Schlegel, K. Eidmann, E. Forster & K. Witte, (2003). Anomalies in high-order harmonic generation at relativistic intensities *Phys. Rev. A*, Vol. 67, pp. 0138161-11
- C. Thaury, F. Quéré, J.-P. Geindre, A. Lévy, T. Cecotti, P. Monot, M. Bougeard, F. Réau, P. D'Oliveira, P. Audebert, R. Marjoribanks & P. Martin, (2007). Plasma mirrors for ultrahigh-intensity optics *Nature Physics*, Vol. 3, pp. 424-429
- R. Toth, J. C. Kieffer, S. Fourmaux, T. Ozaki & A. Krol, (2005). In-line phase-contrast imaging with a laser-based hard x-ray source *Rev. Sci. Instrum.*, Vol. 76, pp. 083701
- R. Toth, S. Fourmaux, T. Ozaki, M. Servol, J. C. Kieffer, R. E. Kincaid & A. Krol, (2007). Evaluation of ultrafast laser-based hard x-ray sources for phase-contrast imaging *Phys. Plasmas*, Vol. 14, pp. 053506-8
- T. Wittmann, J. P. Geindre, P. Audebert, R. S. Marjoribanks, J. P. Rousseau, F. Burgy, D. Douillet, T. Lefrou, K. Ta Phuoc & J. P. Chambaret (2006). Towards ultrahigh-contrast ultraintense laser pulses—complete characterization of a double plasma-mirror pulse cleaner *Rev. Sci. Instrum.*, Vol. 77, pp. 083109-6
- J. Workman, A. Maksimchuk, X. Liu, U. Ellenberger, J. S. Coe, C.-Y. Chien & D. Umstadter, (1996). Picosecond soft-x-ray source from subpicosecond laser-produced plasmas *JOSA B*, Vol. 13, pp. 125-131
- V. Yanovsky, V. Chvykov, G. Kalinchenko *et al.*, (2008). Ultra-high intensity-300 TW laser at 0.1 Hz repetition rate *Opt. Express*, Vol. 16, pp. 2110
- K. Zeil, S. D. Kraft, S. Bock, M. Bussmann, T. E. Cowan, T. Kluge, J. Metzkes, T. Richter, R. Sauerbrey & U. Schramm (2010). The scaling of proton energies in ultrashort pulse laser plasma acceleration *New Journal of Physics*, Vol. 12, pp. 045015 1-16

- A. Zhidkov, A. Sasaki, T. Utsumi, I. Fukumoto, T. Tajima, F. Saito, Y. Hironaka, K. G. Nakamura, K-I Kondo & M. Yoshida, (2000). Prepulse effects on the interaction of intense femtosecond laser pulses with high-Z solids *Phys. Rev. E* Vol. 62, pp. 7232-7240
- A. Zhidkov, J. Koga, A. Sasaki & M. Uesaka, (2002). Radiation Damping Effects on the Interaction of Ultraintense Laser Pulses with an Overdense Plasma *Phys. Rev. Lett.*, Vol. 88, pp. 185002

IntechOpen

IntechOpen



## **Laser Systems for Applications**

Edited by Dr Krzysztof Jakubczak

ISBN 978-953-307-429-0

Hard cover, 308 pages

**Publisher** InTech

**Published online** 14, December, 2011

**Published in print edition** December, 2011

This book addresses topics related to various laser systems intended for the applications in science and various industries. Some of them are very recent achievements in laser physics (e.g. laser pulse cleaning), while others face their renaissance in industrial applications (e.g. CO<sub>2</sub> lasers). This book has been divided into four different sections: (1) Laser and terahertz sources, (2) Laser beam manipulation, (3) Intense pulse propagation phenomena, and (4) Metrology. The book addresses such topics like: Q-switching, mode-locking, various laser systems, terahertz source driven by lasers, micro-lasers, fiber lasers, pulse and beam shaping techniques, pulse contrast metrology, and improvement techniques. This book is a great starting point for newcomers to laser physics.

### **How to reference**

In order to correctly reference this scholarly work, feel free to copy and paste the following:

Sylvain Fourmaux, Stéphane Payeur, Philippe Lassonde, Jean-Claude Kieffer and François Martin (2011). Laser Pulse Contrast Ratio Cleaning in 100 TW Scale Ti: Sapphire Laser Systems, Laser Systems for Applications, Dr Krzysztof Jakubczak (Ed.), ISBN: 978-953-307-429-0, InTech, Available from: <http://www.intechopen.com/books/laser-systems-for-applications/laser-pulse-contrast-ratio-cleaning-in-100-tw-scale-ti-sapphire-laser-systems>

**INTECH**  
open science | open minds

### **InTech Europe**

University Campus STeP Ri  
Slavka Krautzeka 83/A  
51000 Rijeka, Croatia  
Phone: +385 (51) 770 447  
Fax: +385 (51) 686 166  
[www.intechopen.com](http://www.intechopen.com)

### **InTech China**

Unit 405, Office Block, Hotel Equatorial Shanghai  
No.65, Yan An Road (West), Shanghai, 200040, China  
中国上海市延安西路65号上海国际贵都大饭店办公楼405单元  
Phone: +86-21-62489820  
Fax: +86-21-62489821

© 2011 The Author(s). Licensee IntechOpen. This is an open access article distributed under the terms of the [Creative Commons Attribution 3.0 License](#), which permits unrestricted use, distribution, and reproduction in any medium, provided the original work is properly cited.

IntechOpen

IntechOpen